Analyst

Accepted Manuscript

ROYAL SOCIETY OF CHEMISTRY

www.rsc.org/analyst

Use of solid-state nanopores for sensing co-translocational deformation of nano-liposomes

Gaurav Goyal [1], Armin Darvish [1] and Min Jun Kim [1, 2, *]

[1]School of Biomedical Engineering, Science and Health Systems, Drexel University, Philadelphia, PA 19104, United States, [2]Department of Mechanical Engineering and Mechanics, Drexel University, Philadelphia, PA 19104, United States

**Address correspondence to:*
Dr. Min Jun Kim
Associate Professor
Department of Mechanical Engineering and Mechanics
Drexel University,
3141 Chestnut Street, Philadelphia, PA 19104
United States
Email:mkim@coe.drexel.edu
Phone: 215-895-2295

Key Words: Solid-state nanopores, resistive pulse sensing, liposomes, nanoparticles, membrane deformation

Abstract

Membrane deformation of nano-vesicles is crucial in many cellular processes such as virus entry into the host cell, membrane fusion, endo- and exocytosis; however, studying deformation of sub-100 nm soft vesicles is very challenging using the conventional techniques. In this paper, we report detecting co-translocational deformation of individual 1, 2-dioleoyl-sn-glycero-3-phosphocholine (DOPC) nano-liposomes using solid-state nanopore. Electrokinetic translocation through the nanopore caused the soft DOPC liposomes (85 nm diameter) to change shape, which we attribute to the strong electric field strength and physical confinement inside the pore. The experiments were performed at varying transmembrane voltages and the deformation was observed to mount up with increasing applied voltage and followed an exponential decay trend. Numerical simulations were performed to simulate concentrated electric field strength inside the nanopore and a field strength of 14 kV/cm (at 600 mV applied voltage) was achieved at the pore center. The electric field strength inside the nanopore is much higher than the field strength known to cause deformation of 15-30 μm giant membrane vesicles. As a control, we also performed experiments with rigid polystyrene beads that did not show any deformation during translocation events, which further established our hypothesis of co-translocational deformation of liposomes. Our technique presents an innovative and high throughput means for investigating deformation behavior of soft nano-vesicles.

Introduction

Liposomes are artificial nanoscale sacs made up of lipid bilayers that have been widely studied over the past decades as model biological membranes, or as nanocarriers for drug delivery systems [1-6]. These nano-vesicles resemble the physical and mechanical characteristics of biological organelles such as lysosomes, endosomes, exosomes and viruses like human immunodeficiency virus (HIV). Studying the deformability of soft vesicles is of great interest because their mechanical properties play a crucial role in biological phenomena such as membrane fusion, endocytosis, exocytosis and assembly of enveloped viruses. For example, the fusion of biological carriers (vesicles, viruses, exosomes, etc.) with their target cells or organelles directly depends on their ability to deform [7]. Mechanical properties of the lipid bilayer have also been shown to influence biological functions such as fusion and budding [8-10]. Additionally, when using liposomes for delivery of drugs and cosmetics into the skin, their penetration through the epidermis into the deeper skin layers is also directly related to the liposome deformability [11-17]. Despite much effort, current technologies are limited in their ability to study deformation of soft particles at sub-micron levels. While a tremendous body of work exists on giant vesicles and cells (14-30 μm in diameter [18, 19]), experimental data on nanoscale biological carriers (such as viruses, exosomes, etc.) or nano-liposomes are limited. Current single particle techniques used to image or study nano-vesicles include confocal microscopy, electron microscopy, and atomic force microscopy (AFM) [20]. While confocal microscopy can be used to image and study dynamic interactions of sub-micron vesicles, it still cannot resolve structures below 200 nm [20]. On the other hand, electron microscopy can enable us to obtain high resolution images of the nano-vesicles [21]; however, it requires sample fixation and therefore is not suitable for studying dynamics of deformation. Force spectroscopy by AFM is currently the only technique that can characterize mechanical deformation of whole-particles at high resolution. Several researchers have used AFM to study the membrane bending rigidity of liposomes and viruses [10, 22-28]. The main drawback of AFM lies in its low-throughput and the need to immobilize nanoparticles on a surface, which in the case of soft vesicles can cause significant deformation.

Here we report the use of solid-state nanopores for high throughput sensing of liposome deformation at the single particle level. The technique is based on the principle of resistive pulse sensing wherein analyte translocations through a small nanopore are detected based on the current modulations in the circuit. A typical nanopore set-up involves placing a thin insulating membrane, with a solitary nanopore, between two electrolyte chambers. Applying a transmembrane voltage results in a steady ionic current in the circuit whose magnitude depends on the applied voltage, the nanopore diameter and the electrolyte strength. When nanoparticles are added to one of the chambers, they translocate through the pore causing resistive spikes. The magnitude and duration of the resistive spikes (or current blockades) can be used to make inferences about the translocating particles. This technique allows single particle level investigation of nanoparticles at physiological conditions and in the solution state. Moreover, hundreds of nanoparticles can be driven through the pore making nanopore sensing an attractive technique for high throughput characterization of nanoparticles. Although there have been many reports on the use of solid-state nanopores for detection, sizing and separation of rigid non-deformable metallic or polymeric nanoparticles [29-33], this technique has only recently been applied to detection and investigation of co-translocational deformation of soft hydrogel particles and liposomes [34-37]. Holden et al. used conical nanopores embedded in glass capillaries to study translocational dynamics of soft hydrated microgels [34, 35] and multilamellar liposomes [36]. The microgel particles (570 nm radius) were pressure-driven through a nanopore of diameter smaller than those of translocating particles. The translocations resulted in deformation and dehydration of microgels as they squeezed through the nanopore [34, 35]. For liposome translocation, conical pores of variable sizes were used and liposome translocation as a function of nanopore diameter and lipid bilayer transition temperature was studied [36]. When 367 ± 79 nm radius liposomes (5% DPPG/ 95% DPPC, Transition temperature = 41 ^{0}C) were translocated through a 208 nm radius pore (at 10 mmHg pressure), liposome deformation and translocation was observed at high temperatures (T > 47 ^{0}C) where the lipid membrane was highly flexible [36]. Pevarnik et al. reported the use of 12 μm long track-etch PET pores with diameter 540 nm to study deformation of ~300 nm hydrogel particles [37]. They attributed

hydrogel deformation to concentration polarization due to the electric field inside the nanopore and the non-homogeneous pressure distribution along the pore axis.

Most of the reports on studying nano-vesicle deformation by solid-state nanopores have used long conical pores and vesicles larger than 380 nm diameter [34-37]. Although, conical glass nanopores and track-etch PET pores are easy to fabricate, their long pore lengths result in lower sensing resolution compared to the thin silicon nitride nanopores. Moreover, studying translocation behavior and deformability of sub-100 nm soft vesicles is of greater scientific interest because many viruses and majority of the exosomes are < 100 nm in diameter [38-40]. To the best of our knowledge, this is the first report on co-translocational deformation of sub-100 nm liposomes using low aspect solid-state nanopore (pore 200 nm in length and 250 nm in diameter). We use pure DOPC (1, 2-dioleoyl-sn-glycero-3-phosphocholine) liposomes and compare their deformation to rigid polystyrene particles. We chose DOPC liposomes because of their low bending rigidity and easy deformability. The lipid chain melting transition temperature of membranes increases with chain saturation [41] and DOPC contains unsaturated long-chain (18:1) oleic acids inserted at the *sn*-1 and *sn*-2 positions. This unsaturation lowers the DOPC transition temperature to −16.5 ^{0}C [42] and consequently it exists in a fluid like liquid crystalline state (L_{α}) at room temperature [43]. The fluid like state of DOPC makes the liposomes soft and easily deformable. Liposomes (~85 nm in diameter) and polystyrene nanoparticles (~75 nm in diameter) were electrokinetically driven through a 250 nm diameter pore and ionic current modulations caused by translocation events were monitored and analyzed to study their translocation behavior. We observed transmembrane voltage dependent deformation of the liposomes, which followed an exponential decay trend. The voltage responsive behavior of liposomes was observed from 100 – 600 mV applied voltage and no events were observed at voltages higher than 600 mV. We believe the high electric field strength inside the nanopore caused the vesicle to rupture at voltages higher than 600 mV. The polystyrene particles were used as a control analyte and they did not show any deformation at voltages tested. The electrohydrodynamic stress due to the concentrated electric field and the physical confinement inside the nanopore is believed to cause the deformation of the liposomes. We

demonstrate the use of solid-state nanopore for probing deformability of sub-100 nm soft vesicles at single particle level. This technique can be used for high throughput mechanical profiling of artificial and natural nano-vesicles.

Results and Discussion

For nanopore translocation experiments, a 250 nm diameter pore drilled in a 200 nm free standing silicon nitride membrane was used. The nanopore chip was assembled in a flow cell as shown before [31] and the *–cis* and *–trans* chambers were filled with 10 mM KCl. DOPC liposomes (~85 nm in diameter) dispersed in 10 mM KCl were filtered through a 0.2 µm filter and added in the *–cis* chamber of the flow cell and a 200 mV transmembrane voltage was applied (Figure 1a). We use unusually low electrolyte concentration for our experiments to maintain liposome integrity. High KCl concentration results in very high osmotic pressure on liposomes and causes them to rupture. Soon after adding the liposome sample, current drop signals corresponding to liposome translocations were detected. In our experiments, the nanopore diameter is larger than the liposome diameter and liposomes could freely translocate through the pore. Figure 1b shows a typical current versus time signal obtained during liposome translocations and the inset shows details of one of the pulses. The current drop (ΔI) and translocation time (Δt) values of the resistive pulses were extracted and used for further analysis. The majority of the events observed were short ($\Delta t < 0.6\ ms$) with low magnitude current blockades (150 pA < ΔI < 350 pA); however, ~14% events observed were longer with ΔI ranging from 350 pA – 700 pA (Figure 1b & 2a). These longer and deeper events can be attributed to liposomes sticking together during translocation or to the co-events. The liposomes used for translocation experiments were also characterized by transmission electron microscopy (TEM) and dynamic light scattering (DLS) techniques for size determination. Figure 1c shows a representative TEM image of liposomes along with the size histogram. The histogram was prepared by measuring the diameters of liposomes in the TEM images using ImageJ software [44]. The histogram was fitted with a Gaussian function to obtain the mean value of 83.08 ± 5.1 nm. The hydrodynamic diameter of liposomes was measured using Malvern Zetasizer Nano and the size histogram was fitted with a Gaussian function, which

gave the mean diameter of 86.54 ± 30.09 nm (Figure 1d). It should be noted that the discrepancy in TEM and DLS sizes is because DLS measures the hydrodynamic diameter of particles which is slightly larger than the actual diameter.

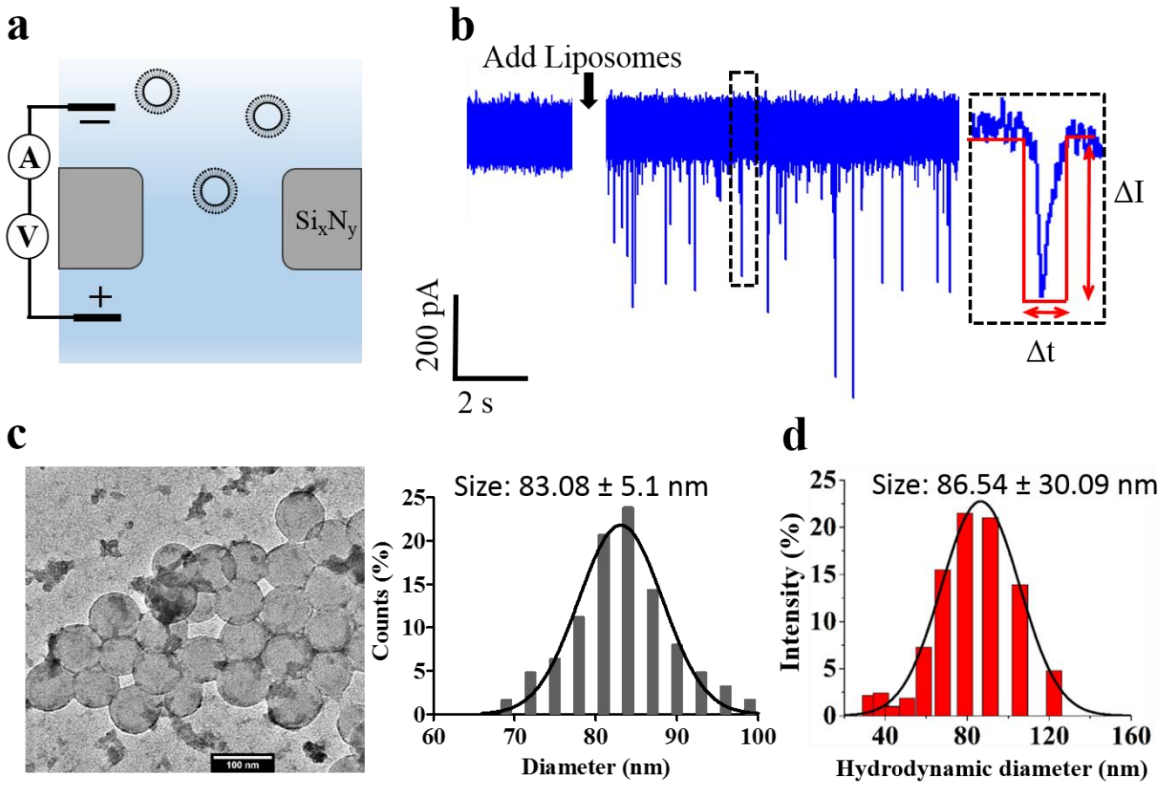

Figure 1. a. Experimental setup. Liposomes were translocated through a 250 nm diameter nanopore drilled in free standing 200 nm thick silicon nitride membrane. b. Representative translocation signals obtained when liposomes were added to the –cis chamber and transmembrane voltage was applied. Inset shows magnified translocation signal and its corresponding current drop and translocation time characteristics. c. TEM image (Scale bar: 100 nm) of liposomes back stained with 2% uranyl acetate and the size histogram obtained from measuring liposome diameter in TEM images. d. Histogram of liposome hydrodynamic diameter measured using dynamic light scattering (DLS).

We recorded and analyzed liposome translocation data at different transmembrane voltages and it revealed a very interesting trend. The events characteristics for experiments at 200 mV and 300 mV were extracted and plotted. As seen in Figure 2a, when the current drop values (ΔI) were plotted against the translocation times (Δt) for the two voltages, we observed a very similar population distribution. In nanopore

experiments, typically, the ΔI values increase with the increasing transmembrane voltage due to an increase in the baseline current value (I_o). The current drop amplitude (ΔI) can be represented in terms of physical properties of the translocating analyte. Based on volume displacement from the pore and neglecting the surface charge effects, we can write [45, 46]:

$$\Delta I = I_o \frac{\Lambda}{H_{eff} A_{pore}} [1 + f(d_{particle}/D_{pore}, L_{particle}/H_{eff})]$$

Where Λ is the excluded volume, H_{eff} is the effective length of the nanopore and $f(d_{particle}/D_{pore}, L_{particle}/H_{eff})$ is the shape correction factor which depends on the diameter of the particle ($d_{particle}$), diameter of the pore (D_{pore}), length of the particle ($L_{particle}$) and effective length of the pore (H_{eff}). We also know that $V_{applied} = I_o R_{pore}$, where $V_{applied}$ is transmembrane voltage, I_o is baseline current and R_{pore} is the resistance of nanopore. If shape and excluded volume of the translocating analyte are constant then $\Delta I \propto V_{applied}$ and in that case ΔI should scale up with the increasing transmembrane voltage. However, we observe that ΔI values remain almost constant despite the increase in I_o when changing applied voltage from 200 mV to 300 mV. In order to rule out the possibility that the non-existent change in ΔI values were due to a small change in the transmembrane voltage, we transformed the ΔI values into percent current drop ($(\Delta I/I_o) \times 100$) values. The histograms were fitted with log-normal distributions to obtain the most probable values. The percent current drop value is directly related to the shape and excluded volume of the translocating analyte and it typically remains constant at different applied voltages if the analyte excluded volume remain the same. Our results show that percent current drop values decreased from a mean value of 8.54 (Std. Dev.: 0.26) to 5.95 (Std. Dev.: 0.24) when the voltage was changed from 200 mV to 300 mV (Figure 2b). An inverse relationship between the percent current drop and the applied voltage suggests co-translocational deformation of liposomes, a phenomenon similar to protein stretching and unfolding during nanopore translocation [47-52]. Our group and others have previously reported that percent current drop (also referred to as normalized

current blockade ratio) decreases as a function of applied voltage due to protein unfolding caused by strong electrical field experienced by proteins inside the solid-state nanopores [47-50]. During nanopore translocation, liposomes also experience high electric field strength inside the pore which may result in concentration polarization and eventual deformation of the soft vesicles. Moreover, electrohydrodynamic forces can exert pressure on the translocating particle and can further aid in vesicle deformation [18, 37].

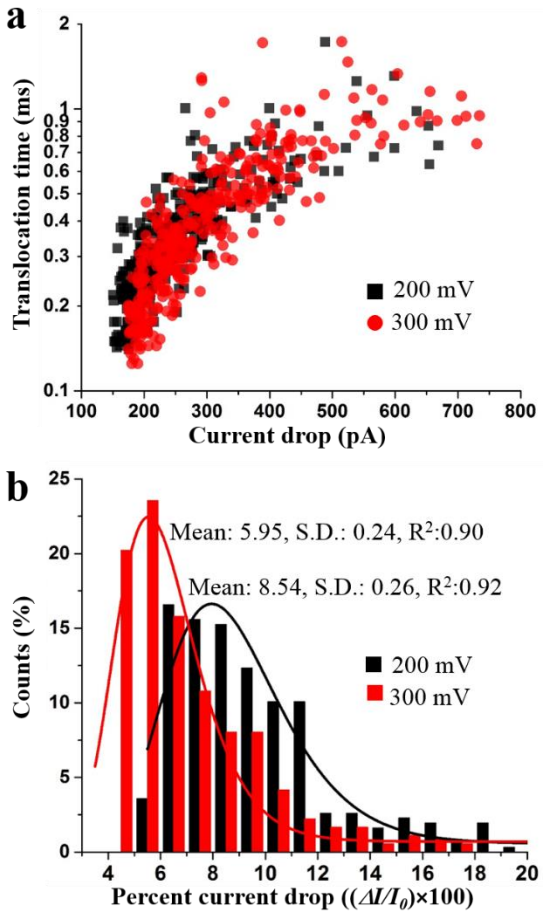

Figure 2. Event characteristics for liposome translocations. a. Scatter plot for current drop versus translocation time at 200 and 300 mV shows very similar population distribution. Translocation time is plotted on log scale. b. Percentage current drop values show a decline with increasing transmembrane voltage suggesting deformation of liposomes during nanopore translocation. N=308 for 200 mV and N=361 for 300 mV. See text for details.

In order to validate our hypothesis, we performed translocation experiments with polystyrene nanoparticles. The Young's modulus of polystyrene is 3 – 3.5 GPa [53], which makes the polystyrene nanoparticles very rigid as compared to liposomes (typical Young's modulus < 100 MPa [22]). The experiments were performed using the same nanopore at 50 mM KCl. We started out by characterizing the nanoparticles using TEM and DLS techniques. Figure 3a shows a representative TEM image of the particles and the size histogram created by measuring the diameters of particles in the TEM images. Figure 3b shows size histogram of the hydrodynamic diameter of the particles measured using DLS. As reported earlier, hydrodynamic diameter was slightly larger than the diameter measured from TEM images.

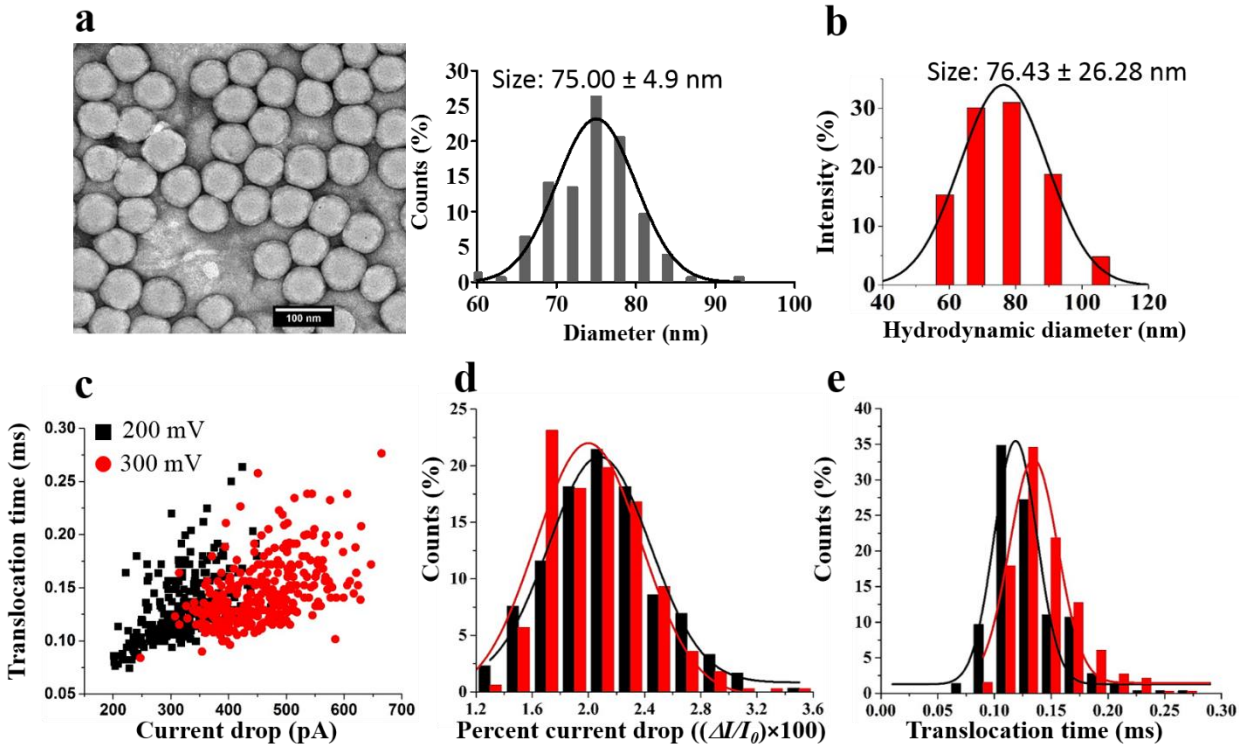

Figure 3. Size and translocation characterization of polystyrene nanoparticles. a. TEM image of polystyrene particles (back stained with 2% uranyl acetate) and the corresponding size histogram. b. Size histogram for the hydrodynamic diameter data obtained by dynamic light scattering (DLS) measurement. c. Current drop (ΔI) versus translocation time (Δt) scatter plot for polystyrene particle translocations at voltages 200 and 300 mV. d. Percentage current drop histograms with Gaussian fits for the two voltages. e. Translocation time histograms for the two voltages. N=303 and 334 for 200 and 300 mV respectively.

For translocation experiments, polystyrene nanoparticles were dispersed in 50 mM KCl and were sonicated for 5 minutes before adding into the *–cis* chamber of the flow cell. When the transmembrane voltage was applied, a stream of translocation events was observed. The current drop values obtained for nanoparticle translocation were regular and more uniform compared to the liposomes, perhaps, because of well dispersed single particle suspension generated after sonication. 50 mM KCl was used for experiments with polystyrene particles instead of 10 mM KCl (used for liposomes) because at 10 mM KCl very low signal to noise ratio was observed and reliable translocation data could not be obtained for voltages < 400 mV (data not shown). Figure 3c shows the scatter plot with current drop values (ΔI) plotted against the translocation times (Δt) for transmembrane voltages of 200 mV and 300 mV. As anticipated, the population cluster shifts with the voltage and we observe higher current drop (ΔI) values at 300 mV compared to 200 mV. The distributions for percentage current drops and translocation times were also plotted and they did not exhibit any significant difference from 200 mV to 300 mV. The peak values for Gaussian curves fit to the percent current drop distributions were 2.07 ± 0.72 and 1.99 ± 0.74 at 200 and 300 mV respectively. As discussed above, $\Delta I/I_o$ = *constant* if the shape and excluded volume of analyte does not change. This translocation behavior of polystyrene particles is similar to what is observed for non-deforming analytes in typical nanopore experiments. Based on our translocation data for both liposomes and polystyrene particles we can conclude that liposomes undergo co-translocational deformation in nanopores.

We directly compare the translocation behavior of liposomes and the polystyrene particles in Figure 4 using a marginal histogram. The event data for the two analytes were plotted for transmembrane voltage of 300 mV. As discussed above, nanoparticles produced events with more uniform current drop values resulting in a tight population distribution. On the other hand, liposomes produced wide population distribution perhaps because of some heterogeneity in the sample. We observe well separated and very distinct population clusters for the two analytes owing to the difference in their hydrodynamic diameters and electrophoretic mobilities. As evident from TEM and DLS characterization of the two analytes, liposomes are roughly 10 nm larger than the polystyrene particles and they are observed to produce deeper current

blockades compared to the polystyrene particles. The percent current drop distributions for the two analytes were fitted with log-normal functions are we obtained peak values of 5.9 (Std. Dev: 0.26) and 1.99 (Std. Dev.: 0.74) for liposomes and polystyrene particles respectively. The electrophoretic velocity of the particles in external electric field (E) is related to their zeta potential ($\xi_{protein}$) by the relation:

$$v = \frac{\varepsilon}{\eta}\xi_{protein}E$$

Where $\varepsilon = \varepsilon_o\varepsilon_r$ and ε_o is dielectric constant and $\varepsilon_r$is permittivity of free space. We measured the zeta-potential for the two analytes and obtained a considerably lower value for liposomes (-8.78 mV) compared to the polystyrene particles (-12.0 mV). The translocation time characteristics of the two analytes is supported by the zeta potential readings, the polystyrene particles with higher zeta potential are expected to have higher electrophoretic velocity and lower translocation time (Peak: 0.13 ms, Std. Dev: 0.17) compared to liposomes (Peak: 0.36 ms, Std. Dev: 0.58), as seen in Figure 4.

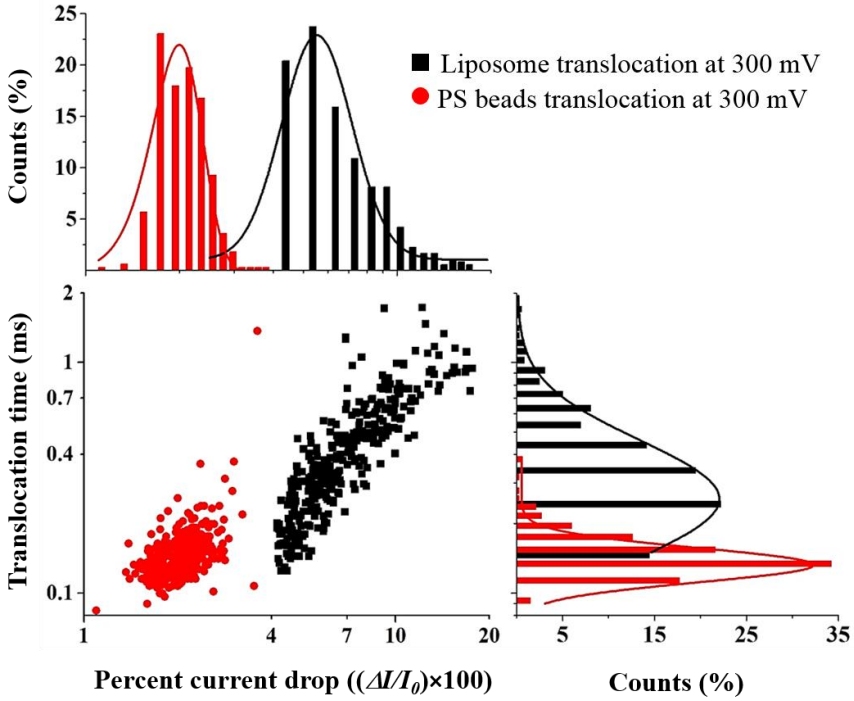

Figure 4. Comparison of translocation behavior of liposomes and polystyrene particles at 300 mV. Both current drop and translocation time in the scatter plot are plotted on log scale.

We performed translocation experiments at a wider range of transmembrane voltages (100 – 600 mV). Although liposome deformation behavior was clearly observed when event distribution at 200 and 300 mV were compared, a wider range of voltages revealed the complete trend. For this analysis, translocation of both the liposomes and the nanoparticles were performed at 100, 200, 300, 400, 500 and 600 mV. We recorded and analyzed 58, 309, 361, 440, 397 and 197 events for liposome translocations and 442, 303, 334, 447, 403 and 130 events for polystyrene translocations at voltages 100 – 600 mV. We extracted the percentage current drop values and plotted their histograms, followed by Gaussian or Log-Normal fitting to the data. The mean and standard deviation values at different voltages obtained from curve fitting were normalized to the values obtained at 100 mV and plotted as a line graph (Figure 5a). We obtained a linear fit to that percentage current drop data for polystyrene particles suggesting no effect of voltage on particle shape, as expected of the rigid nanoparticles. On the other hand, an exponential decay trend ($y = 1.417\, e^{-0.003353x} - 0.028$) is observed for that percentage current drop data for liposome translocation suggesting significant deformation of particles as they translocate through the nanopore. For liposome translocations, additional figures showing the shapes of the resistive pulses, ΔI and Δt histograms, $((\Delta I/I_o) \times 100)$ vs. Δt scatterplot and plot showing inter-event time vs. applied voltages are included in the Supplementary Information.

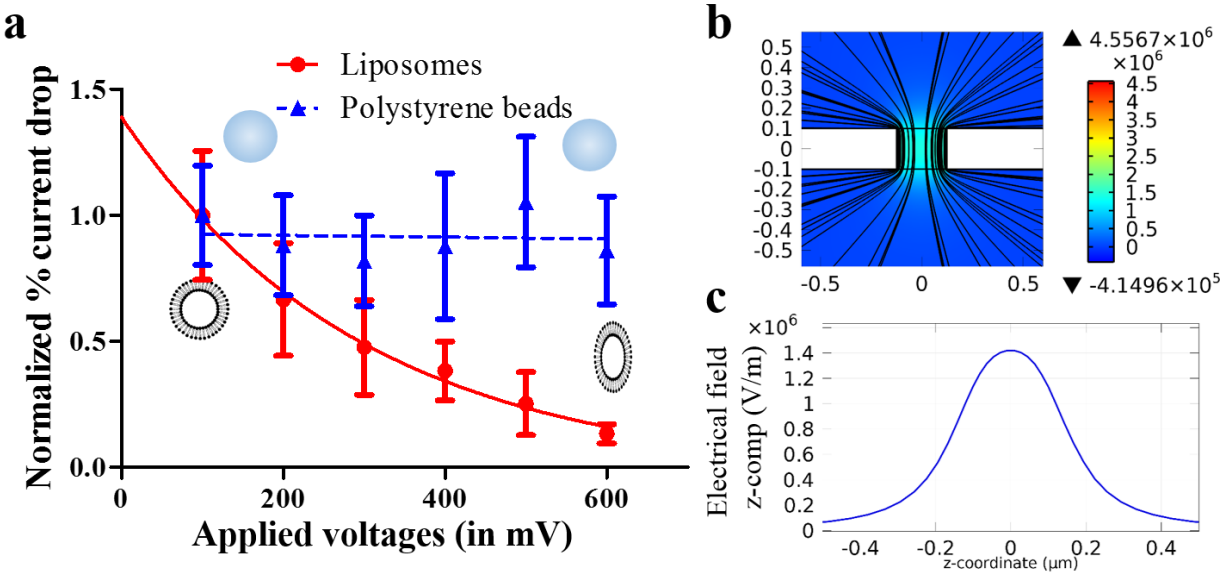

Figure 5. a. Deformation trend observed for liposomes as compared to the polystyrene particles for 100 - 600 mV applied voltages. The rigid polystyrene particles show no deformation whereas liposome follow an exponential trend and their percent current drop values decrease with increasing voltages. b & c. Simulation results for electric field strength inside a nanopore at 600 mV. See text for details.

We also performed mutiphysics simulation using COMSOL to determine the electric field strength inside the nanopore. The simulations were performed with a geometry similar to the dimensions of the nanopore used for translocation experiments. Figure 5b shows the results from the simulation performed at applied voltage of 600 mV. The electric field strength in the geometry is color coded and the rainbow color bar shows majority of electric field concentrated only inside the pore where it reaches a value of 1.46×10^6 V/m at 600 mV transmembrane voltage (Figure 5c). This electric field strength translates to 14 kV/cm which is significantly higher than the electric field strength of 3.0 kV/cm [18] and 2.0 kV/cm [19] reported for deformation of giant vesicles (14 to 30 µm diameter).

The comparison of translocation behavior of liposomes and polystyrene particles was limited to 600 mV because almost no translocation events were observed for liposomes for applied voltages higher than 600 mV. The left panel in Figure 6 shows no liposome translocation was observed at 700 mV but translocation activity was seen when the voltage was lowered to 400 mV, and it again disappeared when the voltage was

raised back to 700 mV. A similar trend was also observed at higher voltages and no reliable translocation data was obtained above 600 mV. On the other hand, translocation events were observed at much higher voltages for polystyrene beads (Figure 6 right panel). We hypothesize that liposomes may be rupturing at voltages higher than 600 mV which prevented their detection.

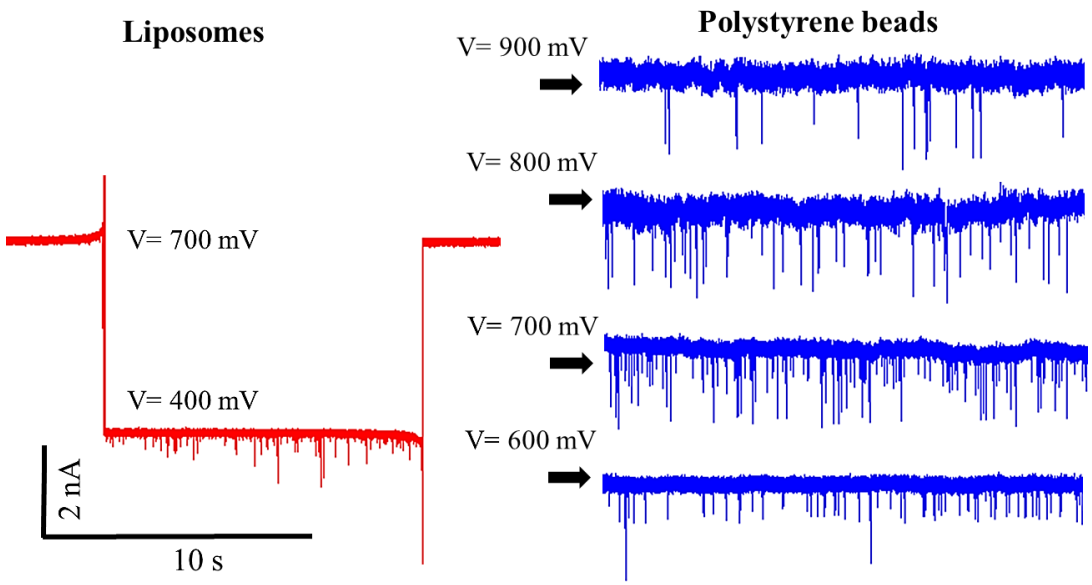

Figure 6. Comparison of translocation activity of liposomes and polystyrene particle at high voltages. For liposomes no activity was seen above 600 mV applied voltage (left panel) whereas polystyrene particles show translocation well above 600 mV.

Experimental

Nanopore fabrication

For nanopore chip fabrication, a 200 nm thick film of silicon nitride (Si_xN_y) was deposited on a 4 inch diameter, 375 μm thick silicon wafer using low pressure chemical vapor deposition (LPCVD). Then using photolithography, Reactive-Ion Etching (RIE), and KOH wet etching a 50 × 50 μm^2 window was fabricated in silicon wafer resulting in 200 nm thick free standing silicon nitride membrane. 250 nm diameter nanopores were then drilled in the Si_xN_y membrane using a FEI Strata DB 235 FIB at an ion beam current of 30 to 50 pA.

Analyte preparation and characterization

1, 2-dioleoyl-sn-glycero-3-phosphocholine (DOPC) liposomes were purchased from FormuMax Scientific Inc. (Palo Alto, CA, USA) and polystyrene particles were purchased from Polysciences Inc. (Warrington, PA, USA). For translocation experiments, liposomes were dispersed in 10 mM KCL (pH 7.0) and were filtered through a 0.2 µm filter to get rid of any aggregates. The polystyrene particles were dispersed in 50 mM KCl and sonicated for 5 minutes before translocation experiments.

For TEM imaging, 5 µl liposome sample was dispensed on a holey carbon TEM grid for 5 minutes, followed by removal of excess liquid by wicking using a filter paper. It was immediately followed by adding 2 µl of 2% uranyl acetate solution to back-stain and preserve the liposomes. The excess staining solution was wicked with a filter paper after 2 minutes and the TEM sample was air dried. The sample was loaded into and imaged using JOEL 2100 TEM operating 120 keV accelerating voltage. A similar sample preparation technique was used for TEM imaging of polystyrene particles and they were imaged under same conditions.

The hydrodynamic diameter of liposomes and polystyrene particles was determined using dynamic light scattering (DLS) device (Zetasizer Nano ZS, Malvern Instruments Ltd.). The intensity-weighted diameters of analytes were recorded, plotted as histogram spikes and fitted with Gaussian distribution. Zeta potential for the two analytes was measured using zeta-potential measuring flow cell provided with the instrument. All measurement data met the quality standards set by Malvern.

Experimental Setup

The nanopore chip was treated with air plasma on either side for 5 minutes to improve wettability. The chip was then sandwiched between two PDMS gaskets and was assembled in a custom built flow cell. The gaskets were filled with electrolyte solution and they served as the -*cis* and the –*trans* chambers. Ag/AgCl electrodes were inserted into the two electrolyte chambers and were connected to a Molecular Devices Axopatch 200B patch clamp amplifier. The current data was sampled at 200 kHz, digitized using a MD Digidata 1440A digitizer, and analyzed using pClamp 10.3 software. Recorded data was pre-conditioned

for analysis by electronic low pass Bessel filtering (10 kHz) and manual baseline correction. A single nanopore chip was used for all the experiments to avoid any bias introduced by pore size variation. After translocation experiment with DOPC liposomes, the nanopore chip was cleaned by dipping in acetone for 5 minutes followed by iso-propyl alcohol and water. The chip was then treated with air plasma (5 minutes each side) and assembled again in the flow cell for experiments with polystyrene particles.

Conclusion

We have demonstrated the use of solid-state nanopores for studying co-translocational deformation of sub-100 nm soft liposomes. Additionally, we show that rigid polystyrene nanoparticles do not deform when subjected to high electric field strengths inside nanopores and can serve as a control analyte for studying deformability of soft vesicles using this technique. This research can be used for high throughput investigation of stability and deformability of nano-vesicles based on their charge, size and lipid composition. This approach of nano-mechanical profiling can also provide insight into design and stability of nanoscale drug carriers.

Acknowledgements

This work was supported by new start-up grant for Dr. Min Jun Kim from Drexel University and NSF Nanomanufacturing Program Award (CMMI #1435000). Authors also thank Dr. Seung-Wook Chi at Korea Research Institute of Bioscience and Biotechnology, South Korea for use of his laboratory facilities and helpful discussion.

Notes and references

1. Bangham, A.D., M.W. Hill, and N.G.A. Miller, *Preparation and use of liposomes as models of biological membranes*. 1974: Springer.
2. Martin, F. and R. Macdonald, *Liposomes can mimic virus membranes.* Nature, 1974. **252**(5479): p. 161-163.

3. Bangham, A.D., M.M. Standish, and J.C. Watkins, *Diffusion of univalent ions across the lamellae of swollen phospholipids.* J. Mol. Biol., 1965. **13**(1): p. 238-252.
4. Malam, Y., M. Loizidou, and A.M. Seifalian, *Liposomes and nanoparticles: nanosized vehicles for drug delivery in cancer.* Trend. Pharmacol. Sci., 2009. **30**(11): p. 592-599.
5. Samad, A., Y. Sultana, and M. Aqil, *Liposomal drug delivery systems: an update review.* Curr. Drug Deliv., 2007. **4**(4): p. 297-305.
6. Schreier, H. and J. Bouwstra, *Liposomes and niosomes as topical drug carriers - dermal and transdermal drug-delivery.* J. Control. Release, 1994. **30**(1): p. 1-15.
7. Chernomordik, L.V. and M.M. Kozlov, *Mechanics of membrane fusion.* Nat. Struct. Mol. Biol., 2008. **15**(7): p. 675-683.
8. Chernomordik, L.V. and M.M. Kozlov, *Protein-lipid interplay in fusion and fission of biological membranes.* Annu. Rev. Biochem., 2003. **72**(1): p. 175-207.
9. Skehel, J.J. and D.C. Wiley, *Receptor binding and membrane fusion in virus entry: the influenza hemagglutinin.* Annu. Rev. Biochem., 2000. **69**(1): p. 531-569.
10. Kol, N., Y. Shi, M. Tsvitov, D. Barlam, R.Z. Shneck, M.S. Kay, and I. Rousso, *A stiffness switch in human immunodeficiency virus.* Biophys. J., 2007. **92**(5): p. 1777-1783.
11. El Maghraby, G.M., A.C. Williams, and B.W. Barry, *Can drug-bearing liposomes penetrate intact skin?* J. Pharmacy Pharmacol., 2006. **58**(4): p. 415-429.
12. Elsayed, M.M., O.Y. Abdallah, V.F. Naggar, and N.M. Khalafallah, *Lipid vesicles for skin delivery of drugs: reviewing three decades of research.* Int. J. Pharmaceutics, 2007. **332**(1-2): p. 1-16.
13. Elsayed, M.M., O.Y. Abdallah, V.F. Naggar, and N.M. Khalafallah, *Deformable liposomes and ethosomes: mechanism of enhanced skin delivery.* Int. J. Pharmaceutics, 2006. **322**(1-2): p. 60-66.
14. Trotta, M., E. Peira, M.E. Carlotti, and M. Gallarate, *Deformable liposomes for dermal administration of methotrexate.* Int. J. Pharmaceutics, 2004. **270**(1-2): p. 119-125.
15. Trotta, M., E. Peira, F. Debernardi, and M. Gallarate, *Elastic liposomes for skin delivery of dipotassium glycyrrhizinate.* Int. J. Pharmaceutics, 2002. **241**(2): p. 319-327.
16. Geusens, B., J. Lambert, S.C. De Smedt, K. Buyens, N.N. Sanders, and M. Van Gele, *Ultradeformable cationic liposomes for delivery of small interfering RNA (siRNA) into human primary melanocytes.* J. Control. Release, 2009. **133**(3): p. 214-220.
17. Dubey, V., D. Mishra, A. Asthana, and N.K. Jain, *Transdermal delivery of a pineal hormone: melatonin via elastic liposomes.* Biomaterials, 2006. **27**(18): p. 3491-3496.
18. Riske, K.A. and R. Dimova, *Electric pulses induce cylindrical deformations on giant vesicles in salt solutions.* Biophys. J., 2006. **91**(5): p. 1778-86.
19. Sadik, M.M., J. Li, J.W. Shan, D.I. Shreiber, and H. Lin, *Vesicle deformation and poration under strong dc electric fields.* Phys. Rev. E Stat. Nonlin. Soft Matter Phys., 2011. **83**(6 Pt 2): p. 066316.
20. Ruozi, B., D. Belletti, A. Tombesi, G. Tosi, L. Bondioli, F. Forni, and M.A. Vandelli, *AFM, ESEM, TEM, and CLSM in liposomal characterization: a comparative study.* Int. J. Nanomedicine, 2011. **6**: p. 557.
21. Almgren, M., K. Edwards, and G. Karlsson, *Cryo transmission electron microscopy of liposomes and related structures.* Colloids Surf., A, 2000. **174**(1): p. 3-21.
22. Li, S., F. Eghiaian, C. Sieben, A. Herrmann, and I.A. Schaap, *Bending and puncturing the influenza lipid envelope.* Biophys. J., 2011. **100**(3): p. 637-645.
23. Schaap, I.A., F. Eghiaian, A. des Georges, and C. Veigel, *Effect of envelope proteins on the mechanical properties of influenza virus.* J. Biol. Chem., 2012. **287**(49): p. 41078-41088.
24. Baclayon, M., G.J.L. Wuite, and W.H. Roos, *Imaging and manipulation of single viruses by atomic force microscopy.* Soft Matter, 2010. **6**(21): p. 5273-5285.
25. Gladnikoff, M. and I. Rousso, *Directly monitoring individual retrovirus budding events using atomic force microscopy.* Biophys. J., 2008. **94**(1): p. 320-326.
26. Kuznetsov, Y.G., J.G. Victoria, W.E. Robinson, Jr., and A. McPherson, *Atomic force microscopy investigation of human immunodeficiency virus (HIV) and HIV-infected lymphocytes.* J. Virology, 2003. **77**(22): p. 11896-11909.

27. Shibata-Seki, T., J. Masai, T. Tagawa, T. Sorin, and S. Kondo, *In-situ atomic force microscopy study of lipid vesicles adsorbed on a substrate.* Thin Solid Films, 1996. **273**(1): p. 297-303.
28. Schonherr, H., J.M. Johnson, P. Lenz, C.W. Frank, and S.G. Boxer, *Vesicle adsorption and lipid bilayer formation on glass studied by atomic force microscopy.* Langmuir, 2004. **20**(26): p. 11600-11606.
29. Arjmandi, N., W. Van Roy, L. Lagae, and G. Borghs, *Measuring the electric charge and zeta potential of nanometer-sized objects using pyramidal-shaped nanopores.* Anal. Chem., 2012. **84**(20): p. 8490-8496.
30. Davenport, M., K. Healy, M. Pevarnik, N. Teslich, S. Cabrini, A.P. Morrison, Z.S. Siwy, and S.E. Létant, *The role of pore geometry in single nanoparticle detection.* ACS Nano, 2012. **6**(9): p. 8366-8380.
31. Goyal, G., K.J. Freedman, and M.J. Kim, *Gold nanoparticle translocation dynamics and electrical detection of single particle diffusion using solid-state nanopores.* Anal. Chem., 2013. **85**(17): p. 8180-8187.
32. Prabhu, A.S., T.Z.N. Jubery, K.J. Freedman, R. Mulero, P. Dutta, and M.J. Kim, *Chemically modified solid state nanopores for high throughput nanoparticle separation.* J. Phys.: Condens. Matter, 2010. **22**(45): p. 454107.
33. Tsutsui, M., S. Hongo, Y. He, M. Taniguchi, N. Gemma, and T. Kawai, *Single-nanoparticle detection using a low-aspect-ratio pore.* ACS Nano, 2012. **6**(4): p. 3499-3505.
34. Holden, D.A., G. Hendrickson, L.A. Lyon, and H.S. White, *Resistive pulse analysis of microgel deformation during nanopore translocation.* J. Phys. Chem. C, 2011. **115**(7): p. 2999-3004.
35. Holden, D.A., G.R. Hendrickson, W.-J. Lan, L.A. Lyon, and H.S. White, *Electrical signature of the deformation and dehydration of microgels during translocation through nanopores.* Soft Matter, 2011. **7**(18): p. 8035-8040.
36. Holden, D.A., J.J. Watkins, and H.S. White, *Resistive-pulse detection of multilamellar liposomes.* Langmuir, 2012. **28**(19): p. 7572-7577.
37. Pevarnik, M., M. Schiel, K. Yoshimatsu, I.V. Vlassiouk, J.S. Kwon, K.J. Shea, and Z.S. Siwy, *Particle deformation and concentration polarization in electroosmotic transport of hydrogels through pores.* ACS Nano, 2013. **7**(4): p. 3720-3728.
38. Grove, J. and M. Marsh, *The cell biology of receptor-mediated virus entry.* J. Cell Biol., 2011. **195**(7): p. 1071-1082.
39. Théry, C., L. Zitvogel, and S. Amigorena, *Exosomes: composition, biogenesis and function.* Nat. Rev. Immunol., 2002. **2**(8): p. 569-579.
40. Keller, S., M.P. Sanderson, A. Stoeck, and P. Altevogt, *Exosomes: from biogenesis and secretion to biological function.* Immunol. Lett., 2006. **107**(2): p. 102-108.
41. Rawicz, W., K. Olbrich, T. McIntosh, D. Needham, and E. Evans, *Effect of chain length and unsaturation on elasticity of lipid bilayers.* Biophys. J., 2000. **79**(1): p. 328-339.
42. Ulrich, A.S., M. Sami, and A. Watts, *Hydration of DOPC bilayers by differential scanning calorimetry.* BBA-Biomembranes, 1994. **1191**(1): p. 225-230.
43. Attwood, S.J., Y. Choi, and Z. Leonenko, *Preparation of DOPC and DPPC supported planar lipid bilayers for Atomic Force Microscopy and Atomic Force Spectroscopy.* Int. J. Mol. Sci., 2013. **14**(2): p. 3514-3539.
44. Abràmoff, M.D., P.J. Magalhães, and S.J. Ram, *Image processing with ImageJ.* Biophotonics Int., 2004. **11**(7): p. 36-43.
45. DeBlois, R. and C. Bean, *Counting and sizing of submicron particles by the resistive pulse technique.* Rev. Sci. Instrum., 1970. **41**(7): p. 909-916.
46. Henriquez, R.R., T. Ito, L. Sun, and R.M. Crooks, *The resurgence of Coulter counting for analyzing nanoscale objects.* Analyst, 2004. **129**(6): p. 478-482.
47. Freedman, K.J., M. Jürgens, A.S. Prabhu, C.W. Ahn, P. Jemth, J.B. Edel, and M.J. Kim, *Chemical, thermal, and electric field-induced unfolding of single protein molecules studied using nanopores.* Anal. Chem., 2011. **83**(13): p. 5137-5144.

48. Freedman, K.J., S.R. Haq, J.B. Edel, P. Jemth, and M.J. Kim, *Single molecule unfolding and stretching of protein domains inside a solid-state nanopore by electric field.* Sci. Rep., 2013. **3**: p. 1638.
49. Cressiot, B., A. Oukhaled, G. Patriarche, M. Pastoriza-Gallego, J.-M. Betton, L.c. Auvray, M. Muthukumar, L. Bacri, and J. Pelta, *Protein transport through a narrow solid-state nanopore at high voltage: experiments and theory.* ACS Nano, 2012. **6**(7): p. 6236-6243.
50. Oukhaled, A., B. Cressiot, L. Bacri, M. Pastoriza-Gallego, J.M. Betton, E. Bourhis, R. Jede, J. Gierak, L. Auvray, and J. Pelta, *Dynamics of completely unfolded and native proteins through solid-state nanopores as a function of electric driving force.* ACS Nano, 2011. **5**(5): p. 3628-3638.
51. Oukhaled, G., J. Mathe, A.L. Biance, L. Bacri, J.M. Betton, D. Lairez, J. Pelta, and L. Auvray, *Unfolding of proteins and long transient conformations detected by single nanopore recording.* Phys. Rev. Lett., 2007. **98**(15): p. 158101.
52. Talaga, D.S. and J. Li, *Single-molecule protein unfolding in solid state nanopores.* J. Am. Chem. Soc., 2009. **131**(26): p. 9287-97.
53. *Elastic properties and Young modulus for some materials*. Available from: http://www.engineeringtoolbox.com/young-modulus-d_417.html.